Acta Cryst E CRYSTALLOGRAPHIC COMMUNICATIONS

ISSN 2056-9890

Racemic mefloquinium chlorodifluoroacetate: crystal structure and Hirshfeld surface analysis

James L. Wardell,[a]‡ Solange M. S. V. Wardell,[b] Mukesh M. Jotani[c] and Edward R. T. Tiekink[d]*

[a]Fundaçaõ Oswaldo Cruz, Instituto de Tecnologia em Fármacos-Far Manguinhos, 21041-250 Rio de Janeiro, RJ, Brazil, [b]CHEMSOL, 1 Harcourt Road, Aberdeen AB15 5NY, Scotland, [c]Department of Physics, Bhavan's Sheth R. A. College of Science, Ahmedabad, Gujarat 380001, India, and [d]Research Centre for Crystalline Materials, School of Science and Technology, Sunway University, 47500 Bandar Sunway, Selangor Darul Ehsan, Malaysia. *Correspondence e-mail: edwardt@sunway.edu.my

Received 21 May 2018
Accepted 23 May 2018

Edited by W. T. A. Harrison, University of Aberdeen, Scotland

‡ Additional correspondence author, e-mail: j.wardell@abdn.ac.uk.

Keywords: crystal structure; Mefloquine; salt; hydrogen bonding; Hirshfeld surface analysis.

CCDC reference: 1844854

Supporting information: this article has supporting information at journals.iucr.org/e

In the racemic title molecular salt, $C_{17}H_{17}F_6N_2O^+\cdot C_2ClF_2O_3^-$ (systematic name: 2-{[2,8-bis(trifluoromethyl)quinolin-4-yl](hydroxy)methyl}piperidin-1-ium chlorodifluoroacetate), the cation, which is protonated at the piperidine N atom, has the shape of the letter, *L*, with the piperidin-1-ium group being approximately orthogonal to the quinolinyl residue [the $C_q-C_m-C_m-N_a$ (q = quinolinyl; m = methine; a = ammonium) torsion angle is 177.79 (18)°]. An intramolecular, charge-assisted ammonium-$N-H\cdots O$(hydroxyl) hydrogen bond ensures the hydroxy-O and ammonium-N atoms lie to the same side of the molecule [$O_h-C_m-C_m-N_a$ (h = hydroxyl) = −59.7 (2)°]. In the crystal, charge-assisted hydroxyl-$O-H\cdots O^-$(carboxylate) and ammonium-$N^+-H\cdots O^-$(carboxylate) hydrogen bonds generate a supramolecular chain along [010]; the chain is consolidated by $C-H\cdots O$ interactions. Links between chains to form supramolecular layers are of the type $C-Cl\cdots\pi$(quinolinyl-C_6) and the layers thus formed stack along the *a*-axis direction without directional interactions between them. The analysis of the calculated Hirshfeld surface points to the dominance of $F\cdots H$ contacts to the surface (40.8%) with significant contributions from $F\cdots F$ (10.5%) and $C\cdots F$ (7.0%) contacts.

1. Chemical context

Practical interest in compounds related to the title salt relates to the biological activity of Mefloquine ([2,8-bis(trifluoromethyl)quinolin-4-yl]-piperidin-2-ylmethanol). This arises when the racemic compound is reacted with HCl: the resulting salt, [(*R**,S*)-(2-{[2,8-bis(trifluoromethyl)quinolin-4-yl](hydroxymethyl)piperidin-1-ium chloride is an anti-malarial drug, being effective against the causative agent, *Plasmodium falciparum* (Maguire *et al.*, 2006). Subsequently, diverse pharmaceutical potential has been disclosed, namely, as anti-bacterial (Mao *et al.*, 2007), anti-mycobacterial (Gonçalves *et al.*, 2012) and as anti-cancer agents (Rodrigues *et al.*, 2014). With the preceding facts in mind, it is not surprising that crystallography has played a key role in establishing the molecular structures of this class of compound. Of particular crystallographic interest has been the characterization of a pair of kryptoracemates of mefloquinium salts in recent years (Jotani *et al.*, 2016; Wardell, Wardell *et al.*, 2016). The phenomenon of kryptoracemic behaviour has been reviewed in the last decade for both organic and coordination compounds (Fábián & Brock, 2010; Bernal & Watkins, 2015).

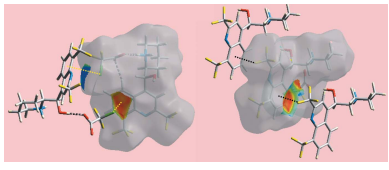

Briefly, for a material to be classified as kryptoracemic, it must satisfy the following crystallographic criteria: the space group must be one of the 65 Sohncke space groups, *i.e.* lacking an inversion centre, rotatory inversion axis, glide plane or a mirror plane, and Z' would usually be greater than 1 (unless the molecule lies on a rotation axis). In a continuation of structural studies of Mefloquine derivatives (Wardell *et al.*, 2011; Wardell, Jotani *et al.*, 2016), herein the crystal and molecular structures of the title salt, (I), isolated from the 1:1 crystallization of racemic Mefloquine and chlorodifluoroacetic acid are described along with an analysis of its calculated Hirshfeld surface.

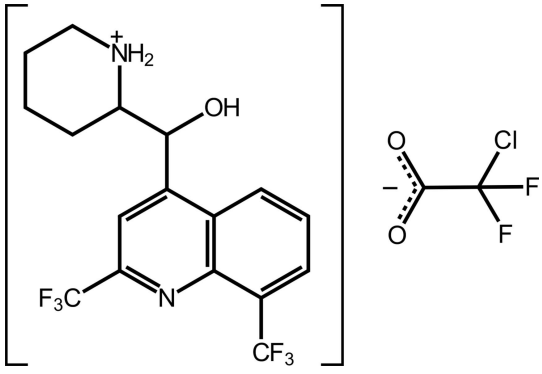

2. Structural commentary

The ions comprising the asymmetric unit of (I) are shown in Fig. 1. The illustrated cation has two chiral centres, namely *R* at C12 and *S* at C13, *i.e.* it is the [(+)-erythro-mefloquinium] isomer. However, it should be noted that the centrosymmetric unit cell has equal numbers of the other *S*-,*R*- enantiomer, indicating that no resolution occurred during the crystallization experiment as has been observed in some of the earlier studies (see *Chemical context*). The pattern of hydrogen-bonding interactions involving the ammonium-N—H H atoms (see *Supramolecular features*) provides confirmation of protonation at the N2 atom during crystallization and, therefore, the formation of a piperidin-1-ium cation. At the same time, delocalization of the π-electron density over the carboxylate residue is confirmed by the equivalence of the C18—O2, O3 bond lengths, *i.e.* 2 × 1.238 (3) Å.

The quinolinyl residue is not strictly planar with the r.m.s. deviation for the ten fitted non-H atoms being 0.0399 Å. This is also reflected in the dihedral angle formed between the (N1,C1–C4,C9) and (C4–C9) rings of 3.95 (15) Å. This aspect of the structure notwithstanding, the hydroxyl-O and ammonium-N atoms lie to opposite sides of the plane through the quinolinyl residue. This is seen in the value of the C2—C3—C12—O1 torsion angle of −20.3 (3)° *cf.* with that of 177.79 (18)° for C3—C12—C13—N2. The latter angle indicates the piperidin-1-ium residue is almost perpendicular to the quinolinyl residue with the methylene-C17 group orientated towards the fused-ring system as seen in the gauche C3—C12—C13—C17 torsion angle of −60.7 (3)°. The observed conformation, whereby the hydroxy-O and ammonium-N atoms lie to the same side of the molecule [the O1—C12—C13—N2 torsion angle is −59.7 (2)°], is stabilized by an intramolecular, charge-assisted ammonium-N2$^+$—H···O1(hydroxyl) hydrogen bond, Table 1. In general terms, the shape of the cation is based on the letter, *L*.

Table 1
Hydrogen-bond geometry (Å, °).

*Cg*1 is the centroid of the (C4–C9) ring.

D—H···*A*	*D*—H	H···*A*	*D*···*A*	*D*—H···*A*
N2—H2*N*···O1	0.89 (2)	2.34 (2)	2.722 (3)	106 (2)
O1—H1*O*···O3^{i}	0.84 (2)	1.83 (2)	2.668 (3)	178 (3)
N2—H1*N*···O2	0.89 (2)	1.92 (2)	2.808 (3)	177 (2)
N2—H2*N*···O2^{ii}	0.89 (2)	2.05 (2)	2.776 (3)	138 (2)
C5—H5···O3	0.95	2.45	3.367 (3)	162
C14—H14*B*···O1^{iii}	0.99	2.39	3.362 (3)	166
C19—Cl1···*Cg*1^{iv}	1.74 (1)	3.91 (1)	4.208 (3)	88 (1)
C10—F3···*Cg*1^{i}	1.33 (1)	3.09 (1)	3.762 (3)	110 (1)

Symmetry codes: (i) $x, y-1, z$; (ii) $-x+1, -y+1, -z+1$; (iii) $x, y+1, z$; (iv) $-x+1, y+\frac{1}{2}, -z+\frac{1}{2}$.

The anion in (I) adopts a conformation where the Cl1 atom lies to one side of the O_2C_2 plane [r.m.s. deviation = 0.0089 Å], with the O2—C18—C19—Cl1 torsion angle being −93.3 (2)°, and the F7 and F8 atoms lying to the other side, the O2—C18—C19—F7, F8 torsion angles = 28.8 (3) and 146.3 (2)°, respectively. The conformation of the $CClF_2$ residue in (I) has been observed in the structure of the acid (Schilling & Mootz, 1995), the acid monohydrate and tetrahydrate (Dahlems *et al.*, 1996) and in salts, *e.g.* with mono-protonated 1,4-diazabicyclo[2.2.2]octane (dabco), *i.e.* 4-aza-1-azoniabicyclo[2.2.2]-octane, for which three independent ion pairs comprise the asymmetric unit (Shi *et al.*, 2013).

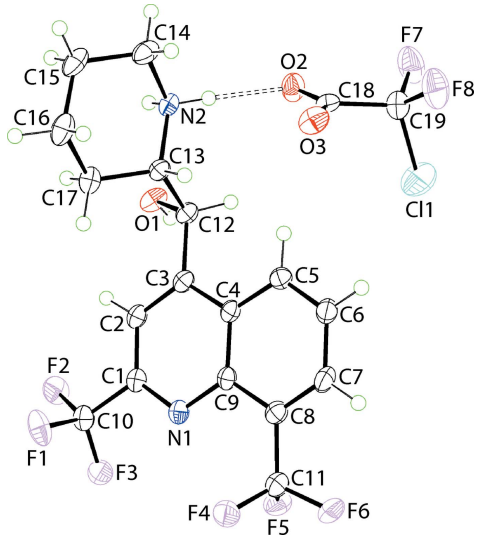

Figure 1
The molecular structures of the ions comprising the asymmetric unit of (I) showing the atom-labelling scheme and displacement ellipsoids at the 70% probability level. The dashed line signifies the N—H···O hydrogen bond.

3. Supramolecular features

The presence of charge-assisted hydroxyl-O—H···O$^-$(carb-(carboxylate) and ammonium-N$^+$—H···O$^-$(carboxylate) hydrogen bonding features prominently in the molecular packing of (I) and leads to a supramolecular chain propagating along the *b*-axis direction, Fig. 1*a* and Table 1. The ammonium-N$^+$—H···O$^-$(carboxylate) hydrogen bonds link two cations and two anions about a centre of inversion to form eight-membered $\{\cdots HNH\cdots O\}_2$ synthons, Fig. 2*b*. These are linked into a supramolecular chain *via* hydroxyl-O—H···O$^-$(carboxylate) hydrogen bonding, which leads to 18-membered $\{\cdots OCO\cdots HNC_2OH\}_2$ synthons, Fig. 2*b*. In this scheme, the carboxylate-O2 atom forms two hydrogen bonds. Additional stability to the supramolecular chain is afforded by quinolinyl-C—H···O(carboxylate) and methylene-C—H···O(hydroxyl) interactions, Table 1. The chains are connected into layers *via* C—Cl···π(C4–C9) interactions, Table 1. The layers stack along the *a*-axis direction without directional interactions between them, Fig. 2*c*.

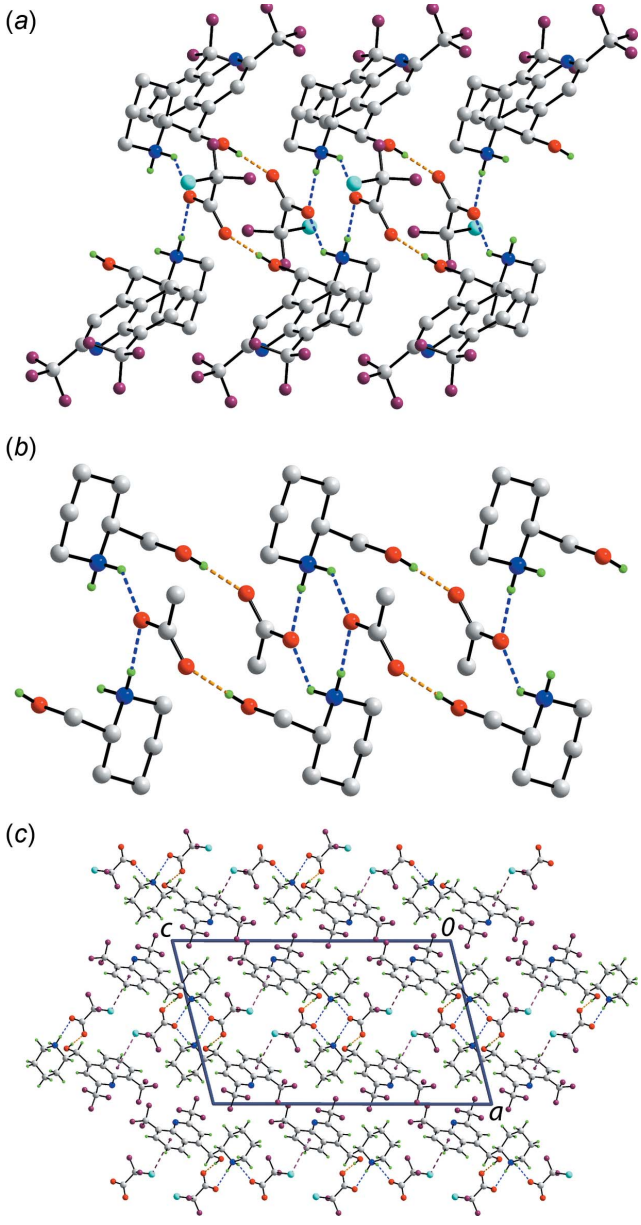

Figure 2
Molecular packing in (I): (*a*) The supramolecular chain along the *b*-axis direction, being sustained by O—H···O and N—H···O hydrogen bonding with non-participating H atoms omitted, (*b*) a simplified view of the chain highlighting the formation of the eight- and 18-membered supramolecular synthons and (*c*) a view of the unit-cell contents shown in projection down the *b*-axis direction. The O—H···O, N—H···O and Cl···π interactions are shown as orange, blue and purple dashed lines, respectively.

Table 2
Summary of short interatomic contacts (Å) in (I).

Contact	Distance	Symmetry operation
H7···H15*B*	2.08	$x, \frac{3}{2}-y, -\frac{1}{2}+z$
F1···H16*B*	2.56	$2-x, 1-y, 1-z$
F6···H15*B*	2.58	$x, \frac{3}{2}-y, -\frac{1}{2}+z$
F4···F5	2.903 (2)	$2-x, \frac{1}{2}+y, 1-z$

4. Hirshfeld surface analysis

The Hirshfeld surface calculations for the title salt (I) were performed in accord with an earlier publication on a related salt (Jotani *et al.*, 2016) and satisfactorily describe the additional influence of interatomic halogen–halogen, halogen–hydrogen and halogen···π contacts upon the packing. In addition to bright-red spots on the Hirshfeld surfaces mapped over d_{norm} in Fig. 3*a* and *b* (labelled 1–3), corresponding to intermolecular O—H···O, N—H···O and C—H···O interactions, Table 1, the presence of tiny faint-red spots, having labels S1–S4 in Fig. 3*c* and *d*, indicate the influence of short

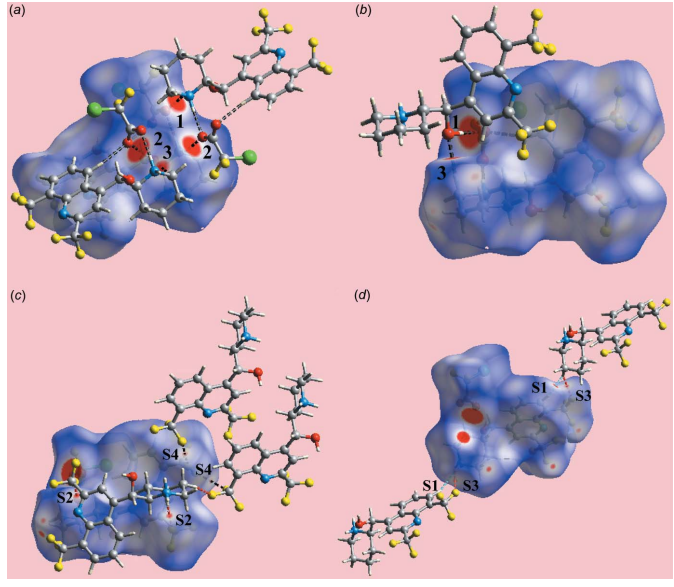

Figure 3
Views of the Hirshfeld surface of (I) mapped over d_{norm} in the range −0.077 to +1.575 au, highlighting: (*a*) and (*b*) intermolecular hydrogen bonds (with labels 1–3) by black-dashed lines, and (*c*) and (*d*) short interatomic H···H, F···H and F···F contacts (with labels S1–S4) by sky-blue, red and black dashed lines, respectively.

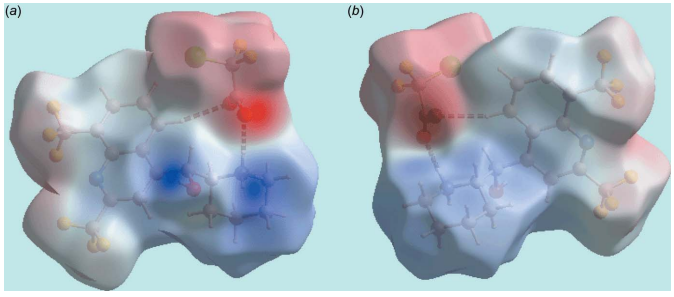

Figure 4
Two views of the Hirshfeld surface of (I) mapped over the electrostatic potential in the range −0.133 to + 0.219 au. The red and blue regions represent negative and positive electrostatic potentials, respectively.

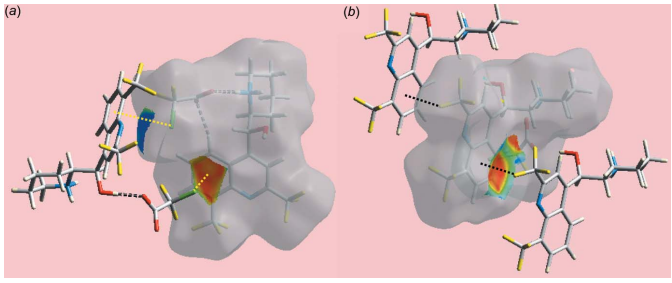

Figure 5
Two views of Hirshfeld surface of (I) mapped over the shape-index property highlighting (*a*) C—Cl···π and (*b*) C—F···π contacts by yellow and black dotted lines, respectively

interatomic H···H, F···H/H···F and F···F contacts [Table 2; calculated in *CrystalExplorer3.1* (Wolff *et al.*, 2012)]. On the Hirshfeld surfaces mapped over electrostatic potential in Fig. 4, the donors and acceptors of intermolecular hydrogen bonds are illustrated through the appearance of blue and red regions corresponding to positive and negative electrostatic potential, respectively. The presence of intermolecular side-on C—halogen···π interactions namely C19—Cl1···π(C4–C9) and C10—F3···π(C4–C9), Table 1, are evident from the Hirshfeld surfaces mapped with shape-index property illustrated in Fig. 5.

Table 3
Percentage contributions of interatomic contacts to the Hirshfeld surface for (I).

	Percentage contribution
Contact	(I)
H···H	11.9
F···H/H···F	40.8
O···H/H···O	11.2
F···F	10.5
C···F/F···C	7.0
Cl···H/H···Cl	4.6
C···H/H···C	3.5
F···Cl/Cl···F	3.1
C···Cl/Cl···C	2.6
N···H/H···N	2.2
C···C	0.6
O···O	0.3
N···F/F···N	0.3
C···N/N···C	0.2
C···O/O···C	0.1
O···Cl/Cl···O	0.1

The overall two-dimensional fingerprint plot and those delineated (McKinnon *et al.*, 2007) into H···H, O···H/H···O, F···H/H···F, F···F, C···F/F···C, Cl···H/H···Cl and C···Cl/Cl···C contacts are illustrated in Fig. 6; the percentage contributions from the different interatomic contacts to the Hirshfeld surface are summarized in Table 3. The formation of a salt between the piperidinium cation and carboxylate anion through the charge-assisted hydrogen bonds and the presence of a number of H···Cl, F and O contacts result in the relatively small, *i.e.* 11.9%, contribution from H···H contacts to the Hirshfeld surface. Conversely, the relative high number of

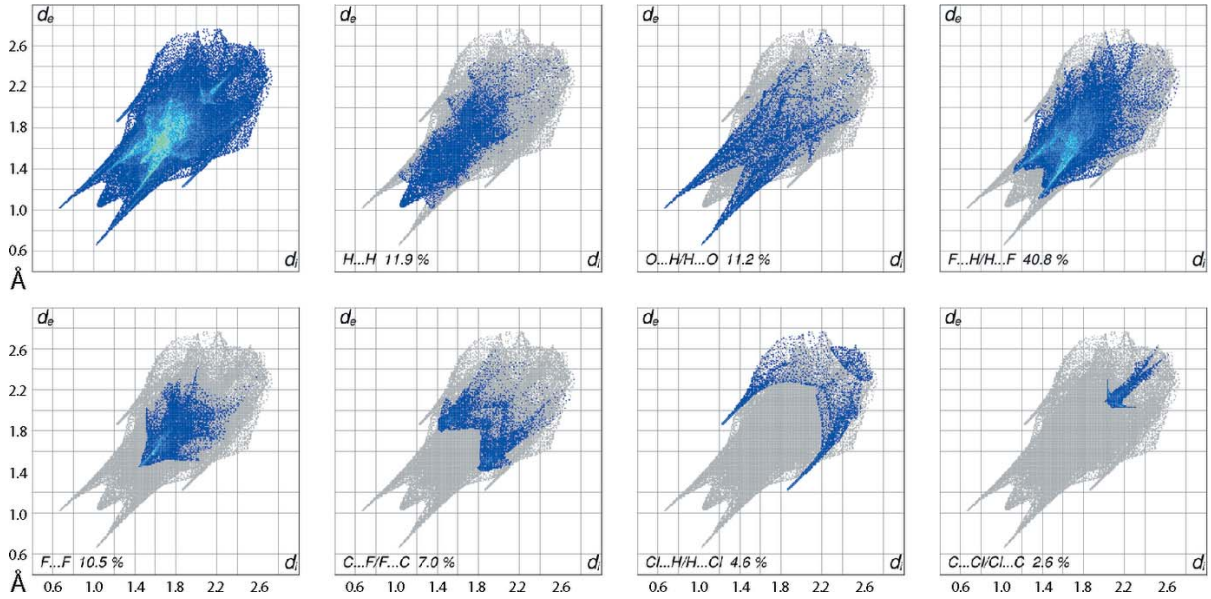

Figure 6
The full two-dimensional fingerprint plot for (I) and those delineated into H···H, O···H/H···O, F···H/H···F, F···F, C···F/F···C, Cl···H/H···Cl and C···Cl/Cl···C contacts.

fluorine atoms lying on the surfaces of both the cation and anion, largely participating in F···H contacts, gives rise to their providing the greatest contribution, *i.e.* 40.8%, to the surface.

In the fingerprint plot delineated into H···H contacts in Fig. 6, the short interatomic H···H contact involving quinoline-H7 and methylene-H15*B*, both derived from the cation, Table 2, is viewed as pencil-like tip at $d_e + d_i$ ~2.0 Å. In the fingerprint plot delineated into O···H/H···O contacts, the spikes associated with the N—H···O hydrogen bonds and C—H···O interactions are merged within the plot. The obvious feature in the plot is a pair of spikes with tips at $d_e + d_i$ ~1.8 Å, which correspond to the most dominant O—H···O hydrogen bond; this is also responsible for most of the points concentrated in the narrower region of spikes. The influence of short interatomic halogen–hydrogen and halogen–halogen contacts in the crystal, Table 2, is observed as a pair of forceps-like tips at $d_e + d_i$ ~2.5 Å (F···H) and 3.0 Å (Cl···H), and an arrow-shaped tip at $d_e + d_i$ ~2.8 Å in the fingerprint plots delineated into F···H/H···F, Cl···H/H···Cl and F···F contacts, respectively. The involvement of chloride and fluoride atoms in C-halogen···π contacts, Table 1, results in the small but significant percentage contribution from C···F/F···C and C···Cl/Cl···C contacts to the Hirshfeld surface, Table 3. These intermolecular contacts are also characterized as forceps-like and anchor-shaped distributions of points in the fingerprint plots delineated into the respective contacts, Fig. 6. The small percentage contribution from other remaining interatomic contacts summarized in Table 3 have negligible effect on the packing in the crystal.

5. Database survey

Kryptoracemic behaviour is rare and is found in only 0.1% of all organic structures (Fábián & Brock, 2010). This observation clearly implies that 99.9% of racemic compounds, molecules with meso symmetry and achiral molecules will crystallize about a centre of inversion. Given there are fewer than 30 structures containing Mefloquine/derivatives of Mefloquine included in the Cambridge Structural Database (Groom *et al.*, 2016), the reporting of two kryptoracemates of mefloquinium cations in recent times (Jotani *et al.*, 2016; Wardell, Wardell *et al.*, 2016) suggests a higher than anticipated propensity for this phenomenon. The two examples were isolated from attempts at chiral resolution of Mefloquine with carboxylic acids. In the first of the two reported structures, the asymmetric unit comprised a pair of pseudo-enantiomeric mefloquinium cations with the charge-balance provided by chloride and 4-fluorobenzenesulfonate anions (Jotani *et al.*, 2016). In the second example, again two mefloquinium cations are pseudo-racemic, with the charge-balance provided by two independent 3,3,3-trifluoro-2-methoxy-2-phenylpropanoate anions, *i.e.* (+)-PhC(CF$_3$)(OMe)CO$_2^-$ (Wardell, Wardell *et al.*, 2016). The appearance of kryptoracemic salts of mefloquinium with non-chiral and chiral counter-ions warrants further investigation into this comparatively rare behaviour in order to reveal the reasons for such crystallization outcomes.

Table 4
Experimental details.

Crystal data	
Chemical formula	$C_{17}H_{17}F_6N_2O^+\cdot C_2ClF_2O_2^-$
M_r	508.79
Crystal system, space group	Monoclinic, $P2_1/c$
Temperature (K)	120
a, b, c (Å)	14.4535 (4), 6.3387 (2), 23.9040 (8)
β (°)	104.214 (2)
V (Å^3)	2122.95 (12)
Z	4
Radiation type	Mo $K\alpha$
μ (mm^{-1})	0.27
Crystal size (mm)	0.62 × 0.20 × 0.06
Data collection	
Diffractometer	Bruker–Nonius Roper CCD camera on κ-goniostat
Absorption correction	Multi-scan (*SADABS*; Sheldrick, 2007)
T_{min}, T_{max}	0.623, 0.746
No. of measured, independent and observed [$I > 2\sigma(I)$] reflections	19411, 4799, 3311
R_{int}	0.054
(sin $\theta/\lambda)_{max}$ (Å^{-1})	0.649
Refinement	
$R[F^2 > 2\sigma(F^2)]$, $wR(F^2)$, S	0.052, 0.142, 1.04
No. of reflections	4799
No. of parameters	307
No. of restraints	3
H-atom treatment	H atoms treated by a mixture of independent and constrained refinement
$\Delta\rho_{max}$, $\Delta\rho_{min}$ (e Å^{-3})	0.94, −0.83

Computer programs: *DENZO* (Otwinowski & Minor, 1997), *COLLECT* (Hooft, 1998), *SHELXS* (Sheldrick, 2008), *SHELXL2014/7* (Sheldrick, 2015), *ORTEP-3 for Windows* (Farrugia, 2012), *DIAMOND* (Brandenburg, 2006) and *publCIF* (Westrip, 2010).

6. Synthesis and crystallization

A solution of mefloquinium chloride (1 mmol) and sodium difluorochoroacetate (1 mmol) in EtOH (10ml) was refluxed for 20 mins. The reaction mixture was left at room temperature and after two days, colourless crystals of the title salt, (I), were collected; M.p. 473–475 K. ^{1}H NMR (DMSO-d_6) δ: 1.20–1.35 (2H, *m*), 1.55–1.75 (4H, *m*), 3.04 (1H, *br t*), 3.53 (1H, *br d*), 5.90 (1H, *s*), 6.94 (1H, *br d*), 8.01 (1H, *t*, *J* = 8.0 Hz), 8.13 (1H, *s*), 8.42 (1H, *d*, *J* = 8.02 Hz), 8.72 (1*H*, *d*, *J* = 8.0 Hz), 9.48 (1H, *br s*); N—H H not observed. ^{13}C NMR (DMSO-d_6) δ: 21.43 (2×), 21.59, 44.51, 58.90, 67.85, 1135.50. 121.17 ($J_{C,F}$ = 273.8 Hz), 121.21 ($J_{C,F}$ = 311.0 Hz), 123.64 ($J_{C,F}$ = 271.7.8 Hz), 126.37, 127.93 ($J_{C,F}$ = 29.2 Hz), 128.32, 128.68. 129.9 ($J_{C,F}$ = 5.2 Hz), 142.78, 146.73 ($J_{C,F}$ = 34.5 Hz), 150.97, 159.82 ($J_{C,F}$ = 25.2 Hz). ^{19}F NMR (DMSO-d_6) δ: −58.65, −58.84, −66.68. IR (cm^{-1}) 3300–2400 (*s*,*v br*), 1662 (*s*).

7. Refinement

Crystal data, data collection and structure refinement details are summarized in Table 4. The carbon-bound H atoms were

placed in calculated positions (C—H = 0.95–1.00 Å) and were included in the refinement in the riding-model approximation, with U_{iso}(H) set to 1.2U_{eq}(C). The O- and N-bound H atoms were refined with the distance restraints O—H = 0.84±0.01 and 0.88±0.01 Å, respectively, and with U_{iso}(H) = 1.5U_{eq}(O) and 1.2U_{eq}(N), respectively.

Acknowledgements

The use of the EPSRC X-ray crystallographic service at the University of Southampton, England, and the valuable assistance of the staff there is gratefully acknowledged.

Funding information

JLW acknowledges support from CNPq (Brazil).

References

Bernal, I. & Watkins, S. (2015). *Acta Cryst.* C**71**, 216–221.
Brandenburg, K. (2006). *DIAMOND*. Crystal Impact GbR, Bonn, Germany.
Dahlems, T., Mootz, D. & Schilling, M. (1996). *Z. Naturforsch. B*, **51**, 536–544.
Fábián, L. & Brock, C. P. (2010). *Acta Cryst.* B**66**, 94–103.
Farrugia, L. J. (2012). *J. Appl. Cryst.* **45**, 849–854.
Gonçalves, R. S. B., Kaiser, C. R., Lourenço, M. C. S., Bezerra, F. A. F. M., de Souza, M. V. N., Wardell, J. L., Wardell, S. M. S. V., Henriques, M., das, G. M. de O. & Costa, T. (2012). *Bioorg. Med. Chem.* **20**, 243–248.
Groom, C. R., Bruno, I. J., Lightfoot, M. P. & Ward, S. C. (2016). *Acta Cryst.* B**72**, 171–179.
Hooft, R. W. W. (1998). *COLLECT*. Nonius BV, Delft, The Netherlands.
Jotani, M. M., Wardell, J. L. & Tiekink, E. R. T. (2016). *Z. Kristallogr.* **231**, 247–255.
Maguire, J. D., Krisin, Marwoto, H., Richie, T. L., Fryauff, D. J. & Baird, J. K. (2006). *Clin. Infect. Dis.* **42**, 1067–1072.
Mao, J., Wang, Y., Wan, B., Kozikowski, A. P. & Franzblau, S. G. (2007). *ChemMedChem*, **2**, 1624–1630.
McKinnon, J. J., Jayatilaka, D. & Spackman, M. A. (2007). *Chem. Commun.* pp. 3814–3816.
Otwinowski, Z. & Minor, W. (1997). *Methods in Enzymology*, Vol. 276, Macromolecular Crystallography, Part A, edited by C. W. Carter Jr & R. M. Sweet, pp. 307–326. New York: Academic Press.
Rodrigues, F. A. R., Bomfim, I. da S., Cavalcanti, B. C., Pessoa, C., Goncalves, R. S. B., Wardell, J. L., Wardell, S. M. S. V. & de Souza, M. V. N. (2014). *Chem. Biol. Drug Des.* **83**, 126–131.
Schilling, M. & Mootz, D. (1995). *J. Fluor. Chem.* **74**, 255–258.
Sheldrick, G. M. (2007). *SADABS*. University of Göttingen, Germany.
Sheldrick, G. M. (2008). *Acta Cryst.* A**64**, 112–122.
Sheldrick, G. M. (2015). *Acta Cryst.* C**71**, 3–8.
Shi, X., Luo, J., Sun, Z., Li, S., Ji, C., Li, L., Han, L., Zhang, S., Yuan, D. & Hong, M. (2013). *Cryst. Growth Des.* **13**, 2081–2086.
Wardell, J. L., Jotani, M. M. & Tiekink, E. R. T. (2016). *Acta Cryst.* E**72**, 1618–1627.
Wardell, S. M. S. V., Wardell, J. L., Skakle, J. M. S. & Tiekink, E. R. T. (2011). *Z. Kristallogr.* **226**, 68–77.
Wardell, J. L., Wardell, S. M. S. V. & Tiekink, E. R. T. (2016). *Acta Cryst.* E**72**, 872–877.
Westrip, S. P. (2010). *J. Appl. Cryst.* **43**, 920–925.
Wolff, S. K., Grimwood, D. J., McKinnon, J. J., Turner, M. J., Jayatilaka, D. & Spackman, M. A. (2012). *CrystalExplorer*. The University of Western Australia.

supporting information

Acta Cryst. (2018). E**74**, 895-900 [https://doi.org/10.1107/S2056989018007703]

Racemic mefloquinium chlorodifluoroacetate: crystal structure and Hirshfeld surface analysis

James L. Wardell, Solange M. S. V. Wardell, Mukesh M. Jotani and Edward R. T. Tiekink

Computing details

Data collection: *COLLECT* (Hooft, 1998); cell refinement: *DENZO* (Otwinowski & Minor, 1997) and *COLLECT* (Hooft, 1998); data reduction: *DENZO* (Otwinowski & Minor, 1997) and *COLLECT* (Hooft, 1998); program(s) used to solve structure: *SHELXS* (Sheldrick, 2008); program(s) used to refine structure: *SHELXL2014/7* (Sheldrick, 2015); molecular graphics: *ORTEP-3 for Windows* (Farrugia, 2012) and *DIAMOND* (Brandenburg, 2006); software used to prepare material for publication: *publCIF* (Westrip, 2010).

2-{[2,8-Bis(trifluoromethyl)quinolin-4-yl](hydroxy)methyl}piperidin-1-ium chlorodifluoroacetate

Crystal data

$C_{17}H_{17}F_6N_2O^+\cdot C_2ClF_2O_2^-$
M_r = 508.79
Monoclinic, $P2_1/c$
a = 14.4535 (4) Å
b = 6.3387 (2) Å
c = 23.9040 (8) Å
β = 104.214 (2)°
V = 2122.95 (12) Å^3
Z = 4
$F(000)$ = 1032
D_x = 1.592 Mg m^{-3}
Mo $K\alpha$ radiation, λ = 0.71073 Å
Cell parameters from 17332 reflections
θ = 2.9–27.5°
μ = 0.27 mm^{-1}
T = 120 K
Lath, colourless
0.62 × 0.20 × 0.06 mm

Data collection

Bruker–Nonius Roper CCD camera on κ-goniostat diffractometer
Radiation source: Bruker–Nonius FR591 rotating anode
Graphite monochromator
Detector resolution: 9.091 pixels mm^{-1}
φ & ω scans
Absorption correction: multi-scan (*SADABS*; Sheldrick, 2007)
T_{min} = 0.623, T_{max} = 0.746
19411 measured reflections
4799 independent reflections
3311 reflections with $I > 2\sigma(I)$
R_{int} = 0.054
θ_{max} = 27.5°, θ_{min} = 3.0°
h = −18→18
k = −8→8
l = −31→30

Refinement

Refinement on F^2
Least-squares matrix: full
$R[F^2 > 2\sigma(F^2)]$ = 0.052
$wR(F^2)$ = 0.142
S = 1.04
4799 reflections
307 parameters
3 restraints
Hydrogen site location: mixed
H atoms treated by a mixture of independent and constrained refinement

$w = 1/[\sigma^2(F_o^2) + (0.0643P)^2 + 1.2072P]$
where $P = (F_o^2 + 2F_c^2)/3$
$(\Delta/\sigma)_{max} < 0.001$

$\Delta\rho_{max} = 0.94$ e Å^{-3}
$\Delta\rho_{min} = -0.83$ e Å^{-3}

Special details

Geometry. All esds (except the esd in the dihedral angle between two l.s. planes) are estimated using the full covariance matrix. The cell esds are taken into account individually in the estimation of esds in distances, angles and torsion angles; correlations between esds in cell parameters are only used when they are defined by crystal symmetry. An approximate (isotropic) treatment of cell esds is used for estimating esds involving l.s. planes.

Fractional atomic coordinates and isotropic or equivalent isotropic displacement parameters (Å²)

	x	*y*	*z*	U_{iso}*/U_{eq}
F1	1.03148 (10)	−0.0703 (2)	0.44433 (7)	0.0399 (4)
F2	0.91566 (11)	−0.2736 (2)	0.44998 (7)	0.0359 (4)
F3	0.96175 (11)	−0.2572 (2)	0.37136 (6)	0.0366 (4)
F4	0.98916 (10)	0.2960 (2)	0.26696 (6)	0.0349 (4)
F5	0.86497 (10)	0.1175 (2)	0.22440 (6)	0.0336 (4)
F6	0.89009 (11)	0.4242 (2)	0.19252 (6)	0.0375 (4)
O1	0.66219 (12)	0.1694 (3)	0.47757 (7)	0.0279 (4)
H1O	0.6352 (19)	0.078 (4)	0.4540 (10)	0.042*
N1	0.88608 (13)	0.1322 (3)	0.34721 (8)	0.0216 (4)
N2	0.64265 (14)	0.5664 (3)	0.51657 (8)	0.0218 (4)
H1N	0.5904 (12)	0.601 (4)	0.4899 (8)	0.026*
H2N	0.6290 (17)	0.450 (3)	0.5335 (10)	0.026*
C1	0.87768 (16)	0.0391 (3)	0.39479 (9)	0.0208 (5)
C2	0.81459 (16)	0.1003 (4)	0.42804 (10)	0.0229 (5)
H2	0.8107	0.0219	0.4613	0.027*
C3	0.75848 (16)	0.2756 (4)	0.41176 (9)	0.0208 (5)
C4	0.76778 (16)	0.3898 (4)	0.36220 (9)	0.0210 (5)
C5	0.71864 (16)	0.5805 (4)	0.34349 (10)	0.0234 (5)
H5	0.6760	0.6371	0.3642	0.028*
C6	0.73220 (17)	0.6835 (4)	0.29583 (10)	0.0264 (5)
H6	0.7007	0.8140	0.2846	0.032*
C7	0.79223 (18)	0.5987 (4)	0.26324 (10)	0.0272 (5)
H7	0.8003	0.6718	0.2301	0.033*
C8	0.83903 (16)	0.4123 (4)	0.27881 (10)	0.0228 (5)
C9	0.83122 (15)	0.3071 (4)	0.33029 (9)	0.0197 (5)
C10	0.94619 (17)	−0.1411 (4)	0.41442 (10)	0.0253 (5)
C11	0.89662 (18)	0.3125 (4)	0.24146 (10)	0.0275 (5)
C12	0.68616 (16)	0.3397 (4)	0.44507 (10)	0.0222 (5)
H12	0.6269	0.3899	0.4171	0.027*
C13	0.72279 (15)	0.5153 (4)	0.48924 (9)	0.0210 (5)
H13	0.7367	0.6430	0.4681	0.025*
C14	0.66441 (19)	0.7397 (4)	0.56031 (10)	0.0296 (6)
H14A	0.6100	0.7582	0.5782	0.036*
H14B	0.6738	0.8737	0.5412	0.036*
C15	0.75362 (19)	0.6874 (4)	0.60653 (10)	0.0323 (6)
H15A	0.7409	0.5645	0.6291	0.039*

H15B	0.7705	0.8086	0.6332	0.039*
C16	0.83715 (19)	0.6373 (4)	0.58047 (11)	0.0322 (6)
H16A	0.8929	0.5940	0.6115	0.039*
H16B	0.8550	0.7654	0.5619	0.039*
C17	0.81136 (17)	0.4608 (4)	0.53591 (10)	0.0266 (5)
H17A	0.8654	0.4364	0.5181	0.032*
H17B	0.8001	0.3288	0.5554	0.032*
C18	0.49744 (17)	0.7909 (4)	0.39729 (10)	0.0227 (5)
C19	0.41892 (18)	0.8393 (4)	0.34241 (11)	0.0322 (6)
Cl1	0.43173 (7)	0.68095 (18)	0.28514 (4)	0.0736 (3)
F7	0.33144 (11)	0.8114 (3)	0.35113 (8)	0.0503 (5)
F8	0.42202 (13)	1.0418 (3)	0.32666 (8)	0.0548 (5)
O2	0.47705 (12)	0.6592 (3)	0.43060 (7)	0.0345 (4)
O3	0.57421 (12)	0.8831 (3)	0.40098 (7)	0.0337 (4)

Atomic displacement parameters (Å²)

	U^{11}	U^{22}	U^{33}	U^{12}	U^{13}	U^{23}
F1	0.0265 (8)	0.0331 (9)	0.0508 (10)	−0.0024 (7)	−0.0085 (7)	0.0049 (7)
F2	0.0410 (9)	0.0275 (8)	0.0417 (9)	0.0037 (7)	0.0150 (7)	0.0167 (7)
F3	0.0443 (9)	0.0331 (8)	0.0319 (8)	0.0130 (7)	0.0087 (7)	−0.0002 (7)
F4	0.0263 (8)	0.0453 (9)	0.0343 (8)	0.0014 (7)	0.0098 (6)	0.0052 (7)
F5	0.0402 (9)	0.0323 (8)	0.0296 (8)	0.0005 (7)	0.0111 (7)	−0.0070 (6)
F6	0.0478 (9)	0.0450 (9)	0.0241 (7)	0.0091 (8)	0.0172 (7)	0.0081 (7)
O1	0.0352 (10)	0.0257 (9)	0.0256 (9)	−0.0125 (8)	0.0129 (8)	−0.0029 (7)
N1	0.0215 (10)	0.0203 (10)	0.0209 (10)	−0.0036 (8)	0.0011 (8)	−0.0009 (8)
N2	0.0257 (11)	0.0225 (11)	0.0166 (9)	−0.0019 (9)	0.0039 (8)	0.0009 (8)
C1	0.0228 (11)	0.0176 (11)	0.0202 (11)	−0.0037 (10)	0.0016 (9)	0.0002 (9)
C2	0.0258 (12)	0.0234 (12)	0.0186 (11)	−0.0041 (10)	0.0040 (9)	0.0027 (10)
C3	0.0219 (12)	0.0217 (12)	0.0180 (11)	−0.0059 (10)	0.0035 (9)	−0.0026 (9)
C4	0.0209 (11)	0.0235 (12)	0.0171 (10)	−0.0023 (10)	0.0021 (9)	−0.0006 (9)
C5	0.0256 (12)	0.0230 (12)	0.0210 (11)	0.0011 (10)	0.0044 (9)	−0.0027 (10)
C6	0.0320 (13)	0.0250 (13)	0.0203 (11)	0.0041 (11)	0.0026 (10)	0.0009 (10)
C7	0.0347 (14)	0.0290 (13)	0.0169 (11)	0.0007 (11)	0.0047 (10)	0.0043 (10)
C8	0.0232 (12)	0.0243 (12)	0.0201 (11)	−0.0033 (10)	0.0037 (9)	−0.0027 (10)
C9	0.0181 (11)	0.0206 (12)	0.0185 (10)	−0.0038 (9)	0.0007 (9)	0.0003 (9)
C10	0.0239 (12)	0.0245 (12)	0.0257 (12)	−0.0036 (10)	0.0024 (10)	0.0023 (10)
C11	0.0304 (14)	0.0294 (13)	0.0236 (12)	0.0004 (11)	0.0080 (10)	0.0044 (11)
C12	0.0246 (12)	0.0229 (12)	0.0202 (11)	−0.0040 (10)	0.0072 (9)	0.0000 (9)
C13	0.0222 (11)	0.0227 (12)	0.0187 (11)	−0.0025 (10)	0.0062 (9)	0.0001 (9)
C14	0.0440 (15)	0.0227 (13)	0.0233 (12)	−0.0020 (11)	0.0108 (11)	−0.0034 (10)
C15	0.0474 (16)	0.0285 (13)	0.0187 (12)	−0.0084 (12)	0.0036 (11)	−0.0049 (10)
C16	0.0377 (14)	0.0314 (14)	0.0229 (12)	−0.0103 (12)	−0.0011 (11)	0.0012 (11)
C17	0.0281 (13)	0.0261 (13)	0.0228 (12)	−0.0036 (11)	0.0012 (10)	0.0020 (10)
C18	0.0257 (12)	0.0232 (12)	0.0210 (11)	0.0006 (10)	0.0089 (10)	−0.0049 (10)
C19	0.0324 (14)	0.0314 (15)	0.0304 (13)	0.0004 (12)	0.0034 (11)	0.0044 (11)
Cl1	0.0796 (6)	0.0932 (8)	0.0373 (5)	0.0119 (6)	−0.0064 (4)	−0.0325 (5)
F7	0.0260 (8)	0.0627 (12)	0.0579 (11)	0.0023 (8)	0.0018 (7)	0.0159 (9)

F8	0.0594 (11)	0.0444 (11)	0.0564 (11)	0.0056 (9)	0.0060 (9)	0.0235 (9)
O2	0.0284 (9)	0.0451 (11)	0.0310 (10)	0.0012 (9)	0.0093 (8)	0.0134 (9)
O3	0.0320 (10)	0.0380 (10)	0.0316 (10)	−0.0117 (9)	0.0085 (8)	−0.0078 (8)

Geometric parameters (Å, º)

F1—C10	1.342 (3)	C7—C8	1.367 (3)
F2—C10	1.344 (3)	C7—H7	0.9500
F3—C10	1.329 (3)	C8—C9	1.428 (3)
F4—C11	1.331 (3)	C8—C11	1.502 (3)
F5—C11	1.346 (3)	C12—C13	1.536 (3)
F6—C11	1.350 (3)	C12—H12	1.0000
O1—C12	1.422 (3)	C13—C17	1.517 (3)
O1—H1O	0.835 (10)	C13—H13	1.0000
N1—C1	1.313 (3)	C14—C15	1.514 (4)
N1—C9	1.365 (3)	C14—H14A	0.9900
N2—C14	1.496 (3)	C14—H14B	0.9900
N2—C13	1.498 (3)	C15—C16	1.522 (4)
N2—H1N	0.888 (10)	C15—H15A	0.9900
N2—H2N	0.886 (10)	C15—H15B	0.9900
C1—C2	1.403 (3)	C16—C17	1.527 (3)
C1—C10	1.509 (3)	C16—H16A	0.9900
C2—C3	1.374 (3)	C16—H16B	0.9900
C2—H2	0.9500	C17—H17A	0.9900
C3—C4	1.423 (3)	C17—H17B	0.9900
C3—C12	1.517 (3)	C18—O2	1.238 (3)
C4—C5	1.418 (3)	C18—O3	1.238 (3)
C4—C9	1.429 (3)	C18—C19	1.540 (3)
C5—C6	1.368 (3)	C19—F8	1.341 (3)
C5—H5	0.9500	C19—F7	1.343 (3)
C6—C7	1.407 (3)	C19—Cl1	1.744 (3)
C6—H6	0.9500		

C12—O1—H1O	107 (2)	F6—C11—C8	111.3 (2)
C1—N1—C9	116.79 (19)	O1—C12—C3	112.03 (19)
C14—N2—C13	114.28 (19)	O1—C12—C13	105.27 (17)
C14—N2—H1N	108.3 (17)	C3—C12—C13	112.92 (18)
C13—N2—H1N	110.7 (17)	O1—C12—H12	108.8
C14—N2—H2N	108.9 (17)	C3—C12—H12	108.8
C13—N2—H2N	107.6 (16)	C13—C12—H12	108.8
H1N—N2—H2N	107 (2)	N2—C13—C17	109.37 (18)
N1—C1—C2	125.3 (2)	N2—C13—C12	106.47 (17)
N1—C1—C10	114.6 (2)	C17—C13—C12	115.3 (2)
C2—C1—C10	120.1 (2)	N2—C13—H13	108.5
C3—C2—C1	118.9 (2)	C17—C13—H13	108.5
C3—C2—H2	120.5	C12—C13—H13	108.5
C1—C2—H2	120.5	N2—C14—C15	110.1 (2)
C2—C3—C4	118.5 (2)	N2—C14—H14A	109.6

C2—C3—C12	120.2 (2)	C15—C14—H14A	109.6
C4—C3—C12	121.3 (2)	N2—C14—H14B	109.6
C5—C4—C3	123.7 (2)	C15—C14—H14B	109.6
C5—C4—C9	118.8 (2)	H14A—C14—H14B	108.1
C3—C4—C9	117.5 (2)	C14—C15—C16	111.5 (2)
C6—C5—C4	120.4 (2)	C14—C15—H15A	109.3
C6—C5—H5	119.8	C16—C15—H15A	109.3
C4—C5—H5	119.8	C14—C15—H15B	109.3
C5—C6—C7	120.8 (2)	C16—C15—H15B	109.3
C5—C6—H6	119.6	H15A—C15—H15B	108.0
C7—C6—H6	119.6	C15—C16—C17	110.9 (2)
C8—C7—C6	120.7 (2)	C15—C16—H16A	109.5
C8—C7—H7	119.6	C17—C16—H16A	109.5
C6—C7—H7	119.6	C15—C16—H16B	109.5
C7—C8—C9	120.0 (2)	C17—C16—H16B	109.5
C7—C8—C11	120.8 (2)	H16A—C16—H16B	108.1
C9—C8—C11	119.2 (2)	C13—C17—C16	111.3 (2)
N1—C9—C4	122.8 (2)	C13—C17—H17A	109.4
N1—C9—C8	118.1 (2)	C16—C17—H17A	109.4
C4—C9—C8	119.0 (2)	C13—C17—H17B	109.4
F3—C10—F1	106.86 (19)	C16—C17—H17B	109.4
F3—C10—F2	106.77 (19)	H17A—C17—H17B	108.0
F1—C10—F2	105.88 (19)	O2—C18—O3	128.6 (2)
F3—C10—C1	113.66 (19)	O2—C18—C19	116.1 (2)
F1—C10—C1	111.04 (19)	O3—C18—C19	115.3 (2)
F2—C10—C1	112.17 (19)	F8—C19—F7	105.5 (2)
F4—C11—F5	107.2 (2)	F8—C19—C18	111.2 (2)
F4—C11—F6	106.65 (19)	F7—C19—C18	111.5 (2)
F5—C11—F6	105.81 (19)	F8—C19—Cl1	108.24 (18)
F4—C11—C8	113.7 (2)	F7—C19—Cl1	109.36 (19)
F5—C11—C8	111.7 (2)	C18—C19—Cl1	110.85 (18)

C9—N1—C1—C2	2.6 (3)	N1—C1—C10—F2	−158.96 (19)
C9—N1—C1—C10	−174.73 (19)	C2—C1—C10—F2	23.6 (3)
N1—C1—C2—C3	−2.4 (3)	C7—C8—C11—F4	117.4 (2)
C10—C1—C2—C3	174.7 (2)	C9—C8—C11—F4	−64.5 (3)
C1—C2—C3—C4	−0.9 (3)	C7—C8—C11—F5	−121.2 (2)
C1—C2—C3—C12	177.0 (2)	C9—C8—C11—F5	57.0 (3)
C2—C3—C4—C5	−175.6 (2)	C7—C8—C11—F6	−3.1 (3)
C12—C3—C4—C5	6.5 (3)	C9—C8—C11—F6	175.05 (19)
C2—C3—C4—C9	3.7 (3)	C2—C3—C12—O1	−20.3 (3)
C12—C3—C4—C9	−174.2 (2)	C4—C3—C12—O1	157.6 (2)
C3—C4—C5—C6	179.0 (2)	C2—C3—C12—C13	98.3 (2)
C9—C4—C5—C6	−0.3 (3)	C4—C3—C12—C13	−83.8 (3)
C4—C5—C6—C7	2.4 (4)	C14—N2—C13—C17	56.2 (3)
C5—C6—C7—C8	−0.6 (4)	C14—N2—C13—C12	−178.61 (18)
C6—C7—C8—C9	−3.3 (4)	O1—C12—C13—N2	−59.7 (2)
C6—C7—C8—C11	174.9 (2)	C3—C12—C13—N2	177.79 (18)

C1—N1—C9—C4	0.6 (3)	O1—C12—C13—C17	61.8 (2)
C1—N1—C9—C8	179.8 (2)	C3—C12—C13—C17	−60.7 (3)
C5—C4—C9—N1	175.6 (2)	C13—N2—C14—C15	−55.7 (3)
C3—C4—C9—N1	−3.7 (3)	N2—C14—C15—C16	54.0 (3)
C5—C4—C9—C8	−3.5 (3)	C14—C15—C16—C17	−55.1 (3)
C3—C4—C9—C8	177.2 (2)	N2—C13—C17—C16	−55.3 (3)
C7—C8—C9—N1	−173.9 (2)	C12—C13—C17—C16	−175.15 (19)
C11—C8—C9—N1	7.9 (3)	C15—C16—C17—C13	56.0 (3)
C7—C8—C9—C4	5.3 (3)	O2—C18—C19—F8	146.3 (2)
C11—C8—C9—C4	−172.9 (2)	O3—C18—C19—F8	−36.6 (3)
N1—C1—C10—F3	−37.7 (3)	O2—C18—C19—F7	28.8 (3)
C2—C1—C10—F3	144.8 (2)	O3—C18—C19—F7	−154.0 (2)
N1—C1—C10—F1	82.8 (2)	O2—C18—C19—Cl1	−93.3 (2)
C2—C1—C10—F1	−94.7 (3)	O3—C18—C19—Cl1	83.9 (2)

Hydrogen-bond geometry (Å, º)

Cg1 is the centroid of the (C4–C9) ring.

D—H···*A*	*D*—H	H···*A*	*D*···*A*	*D*—H···*A*
N2—H2*N*···O1	0.89 (2)	2.34 (2)	2.722 (3)	106 (2)
O1—H1*O*···O3^{i}	0.84 (2)	1.83 (2)	2.668 (3)	178 (3)
N2—H1*N*···O2	0.89 (2)	1.92 (2)	2.808 (3)	177 (2)
N2—H2*N*···O2^{ii}	0.89 (2)	2.05 (2)	2.776 (3)	138 (2)
C5—H5···O3	0.95	2.45	3.367 (3)	162
C14—H14*B*···O1^{iii}	0.99	2.39	3.362 (3)	166
C19—Cl1···*Cg*1^{iv}	1.74 (1)	3.91 (1)	4.208 (3)	88 (1)
C10—F3···*Cg*1^{i}	1.33 (1)	3.09 (1)	3.762 (3)	110 (1)

Symmetry codes: (i) *x*, *y*−1, *z*; (ii) −*x*+1, −*y*+1, −*z*+1; (iii) *x*, *y*+1, *z*; (iv) −*x*+1, *y*+1/2, −*z*+1/2.